Clay Mineralogy and Pore-Scale Characterization During and After CO_2 Flow and Saturation in the Mt. Simon Sandstone, Illinois Basin, USA

Jared T. Freiburg[1, 2], John K. Tudek[3], Shane K. Butler[2], Peter M. Berger[2], Georg H. Grathoff[1]

[1]Institut für Geographie und Geologie, Ernst-Moritz-Arndt Universität Greifswald, Germany, freiburg@illinois.edu
[2]Illinois State Geological Survey, University of Illinois at Urbana-Champaign, Illinois, USA
[3]National Energy Technology Laboratory, U.S. Department of Energy, Morgantown, West Virginia, USA

Background

The Cambrian-age Lower Mt. Simon Sandstone serves as the reservoir for the Illinois Basin - Decatur Project (IBDP), a 1 million tonne carbon capture and storage demonstration project located in Decatur, Illinois, USA. Authigenic illite is the most prevalent clay mineral in the Mt. Simon and most commonly forms a thin coating over detrital quartz grains. This clay coating acted as a barrier to the early authigenic quartz precipitation and thus preserving abundant primary porosity. However, in the Lower Mt. Simon Sandstone, clay minerals variably clog pore throats decreasing reservoir permeability. To predict the fate of CO_2 and its long term effect on reservoir properties, CO_2-water-rock interaction experiments are being completed.

Mt. Simon Sandstone

The Cambrian-age Mt. Simon Sandstone is over 700 m thick in areas of Illinois (Fig. 1). With porosity reaching 27% and permeability up to 1 Darcy, the Lower Mt. Simon is being used as a reservoir to demonstrate carbon dioxide storage that may ultimately lead to zero-emissions power plants.

The Lower Mt. Simon is comprised of braided river deposits dominated by fine to medium grain sub-arkosic sandstone (Fig. 2). A major control on porosity and permeability in the sandstone is clay mineral cementation (Fig. 3). Alteration of clay minerals (i.e. swelling, dissolution) is critical in understanding the fate of the reservoir during and after CO_2 injection.

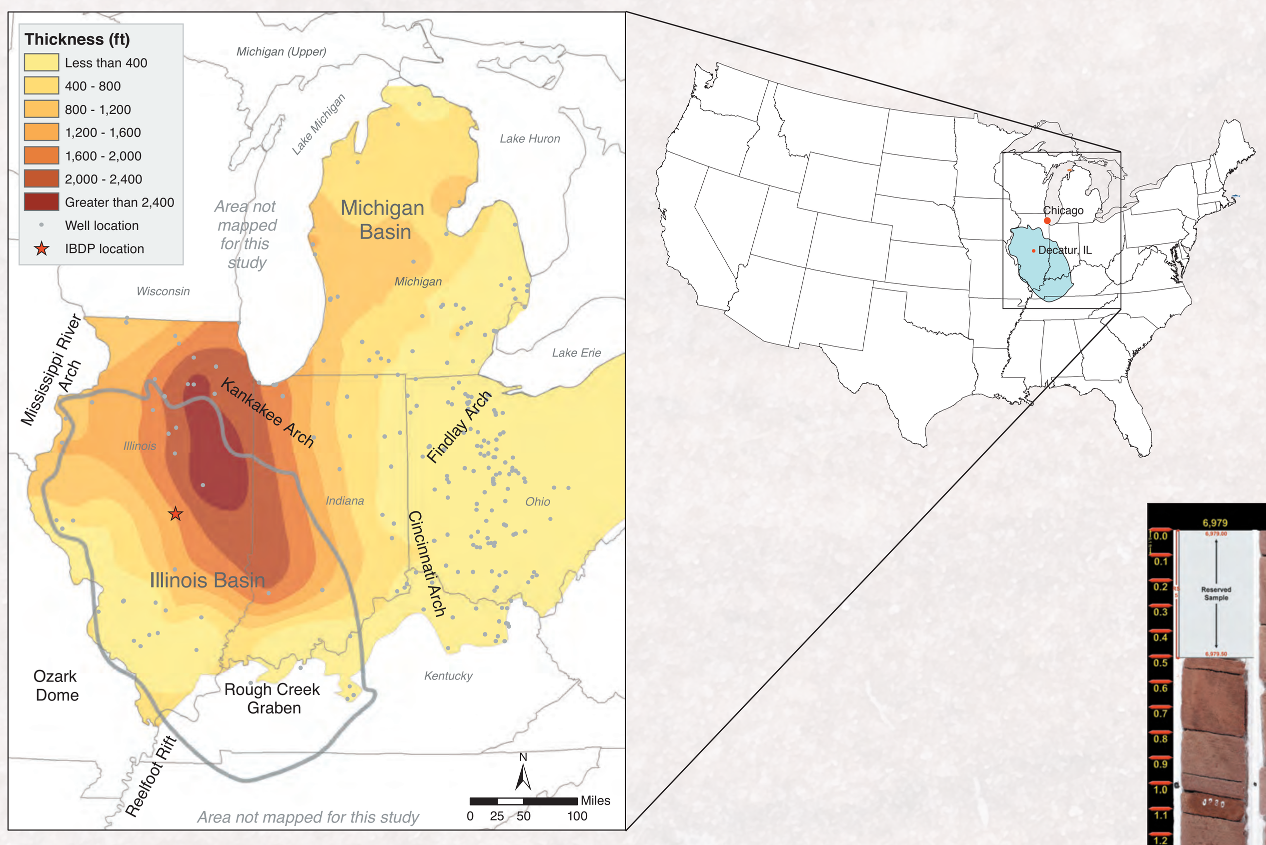

Figure 1. Isopach map of the Mt. Simon Sandstone with red star indicating the location of the Illinois Basin Decatur Project (IBDP).

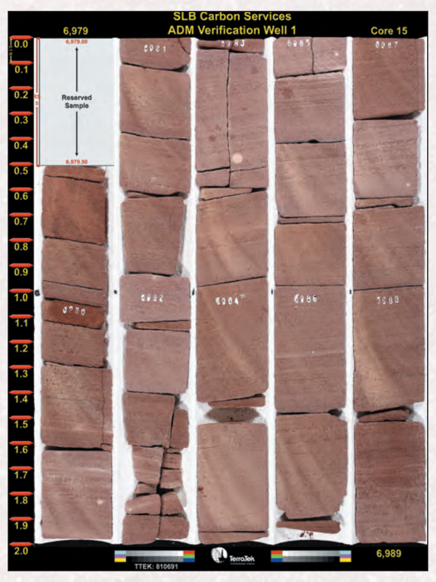

Figure 2. Mt. Simon Sandstone core (10 cm diameter) within the IBDP injection zone.

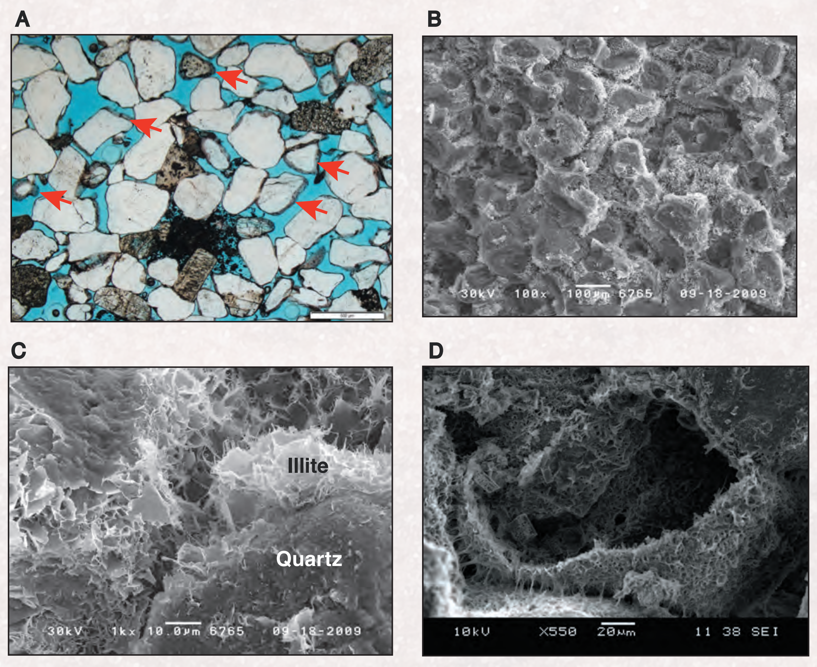

Figure 3. A: Thin section photomicrograph of the sub-arkosic Lower Mt. Simon Sandstone. Notice abundant clay coatings over grains indicated by red arrows. B: SEM photomicrograph of the Lower Mt. Simon Sandstone. Notice abundant clay coatings over grains, filling pore space, and clogging pore throats. C: SEM photomicrograph showing illite coating a detrital quartz grain. D: SEM photomicrograph showing illite coating over a partially to nearly dissolved k-feldspar grain.

Figure 4. Preparing Parr pressure vessel for five month CO_2-brine-rock reaction experiment.

	Dissolution/Precipitation Rates (mole/m2/s)	
	Observed rate (50°C)	Adjusted rate (17°C)
Smectite	9.55E-07	2.17E-07
Illite	9.31E-07	5.15E-07
Kaolinite	8.03E-07	3.76E-07
Chlorite	5.81E-07	1.40E-08
Quartz	3.80E-12	9.28E-14
K-feldspar	8.04E-08	9.01E-09

Table 1. Dissolution rates (Lasaga, 1995; Yoksoulian et al., 2013) based on Parr pressure experiment conditions (50°C) and flow through experiment (17°C).

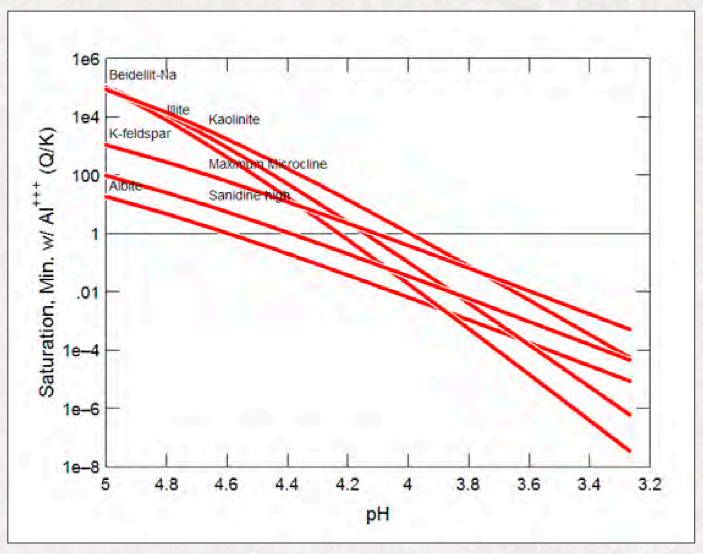

Figure 5. The modeled saturation state of silica and aluminum bearing minerals (Bethke, 1996; Storn and Price, 1997) in an experiment on the Mt. Simon sandstone vs pH. During brine and CO_2 interaction, pH is expected to decrease, and all feldspar and clay minerals are expected to be undersaturated and prone to dissolution.

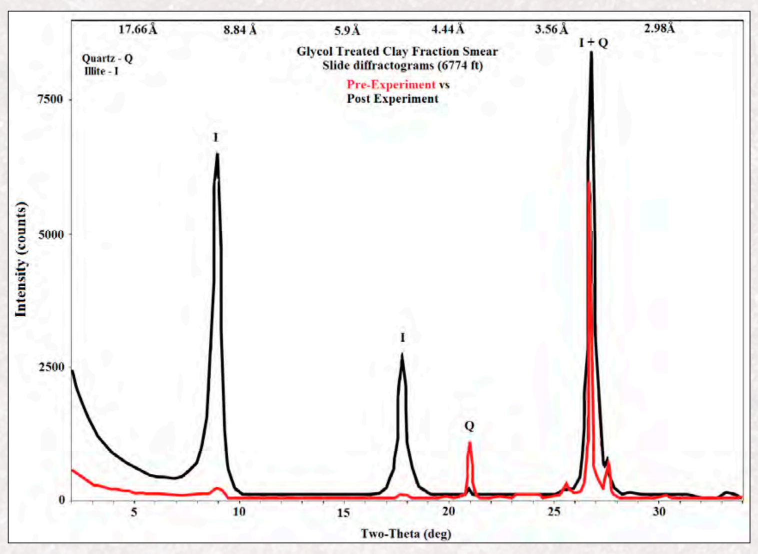

Figure 6. Overlay of pre- and post-experiment glycol treated diffractograms of sample from the same depth (6,774 feet). The pre-experiment (red) has broad illite peaks, possibly from thin illite crystallites with sharp quartz peaks. The post experiment diffractogram (black) has sharp illite peaks, (thick crystallites with shorter quartz peaks (Moore & Reynolds 1997).

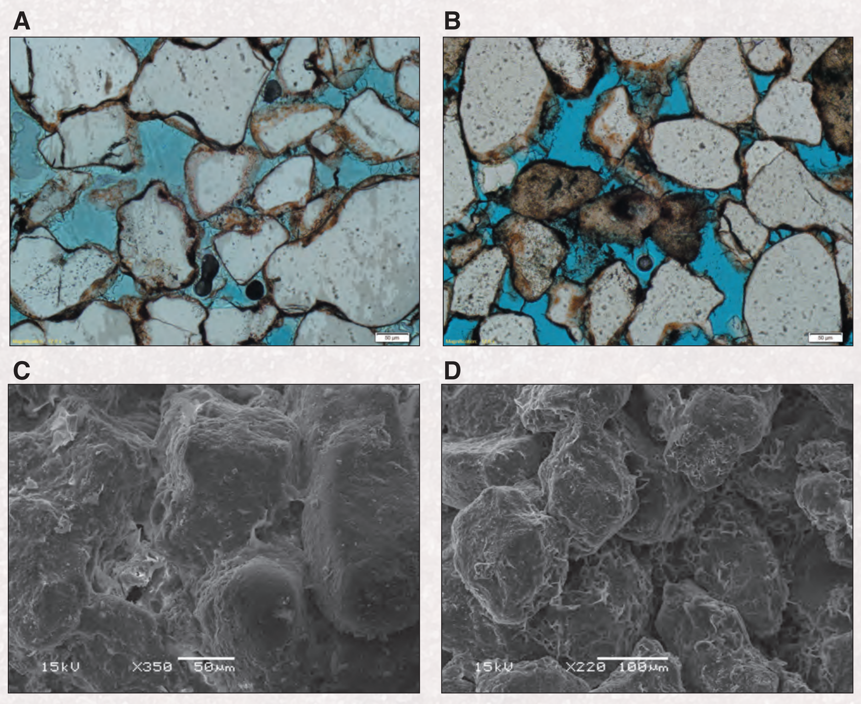

Figure 7. A: Thin section photomicrograph before CO_2 interaction. B. Thin section photomicrograph after CO_2 interaction. C: SEM photomicrograph before CO_2 interaction. D: SEM photomicrograph after CO_2 interaction.

Experimental Procedure

To understand CO_2-brine-rock interaction, experiments were completed in Parr pressure vessels (Fig. 4). CO_2-brine-rock was reacted at reservoir pressure (3,000 psi) and temperature (50°C) for 5 months. Geochemical modeling suggested clay minerals and feldspar would react with a lower pH brine after CO_2 injection (Table 1 and Fig. 5). Pre-experiment XRD analyses indicated that the sandstone samples were composed of quartz, k-feldspar, and illite (Fig. 6). Pre- and post-experiment characterization of the sample was completed with little changes observed in thin sections (Fig. 7A and B) and major changes observed using SEM imaging (Fig. 7C and D). Under SEM, clay minerals in pore space and throats in the post-experiment sample appear to have been dissolved as suggested by brine analyses (Table 2).

		Brine Before	After 1	After 2	After 3	After 4	After 5
Br	mg/L	na	na	10.2	39.5	21.2	13.2
Cl	mg/L	102,202	109,030	109,033	105,413	108,975	109,625
NO3	mg/L	na	na	5	5.27	na	2.06
SO4	mg/L	na	na	na	14.7	53.3	5.09
Al	mg/L	na	0.785	1.2	1.73	0.039	1.76
B	mg/L	17.9	23.5	23.4	26.3	22.8	23.4
Ba	mg/L	na	0.22	0.2	0.74	0.2	0.2
Ca	mg/L	16,495	16,249	15,863	16,131	15,978	16,397
K	mg/L	10,016	9,714	10,029	9,874	10,049	9,992
Li	mg/L	21.5	20.3	20	20.7	20.2	20.3
Mg	mg/L	1,718	1,623	1,599	1,543	1,639	1,630
Mn	mg/L	na	1.17	1.93	1.84	5.24	1.38
Na	mg/L	37,846	37,228	37,690	37,294	37,893	37,754
P	mg/L	na	0.2	0.09	<0.07	0.13	0.16
S	mg/L	na	2.98	2.58	3.3	4.08	3.3
Se	mg/L	na	0.49	0.45	0.77	0.52	0.44
Si	mg/L	na	6.06	10.6	9.93	10.3	12.3
Sr	mg/L	646	564	566	604	569	571

Table 2. Elemental analysis of brine before CO_2-rock reaction and subsequent months into experiment.

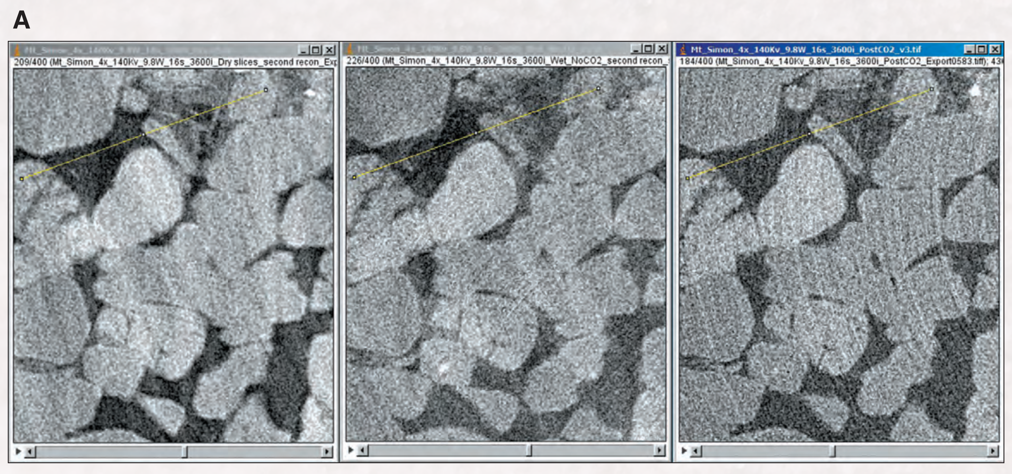

Fig 8) A: MicroCT image slices of sample dry, DI water saturated, and post-CO_2-DI water flow through (from left to right). Pore space is black with clay fill as a dark gray. Notice an increase in clays in the DI water saturated slices and an increase in pore space in post-CO_2-DI water flow through slices. B: The same MicroCT images as Fig. 8A with clays colored (green) in the lower half of the images to illustrate changes in porosity. C: Plotted gray-scale values across profile (yellow line) on MicroCT image slices. Porosity has an interpreted grayscale value below approximately 10,000, clays between 10,000 and 12,000, and detrital grain matrix above 12,000. Notice the changes in porosity and clays between the three scans. This greyscale comparison is unreliable as tomographic images produced by x-rays have variable greyscale in separate scans.

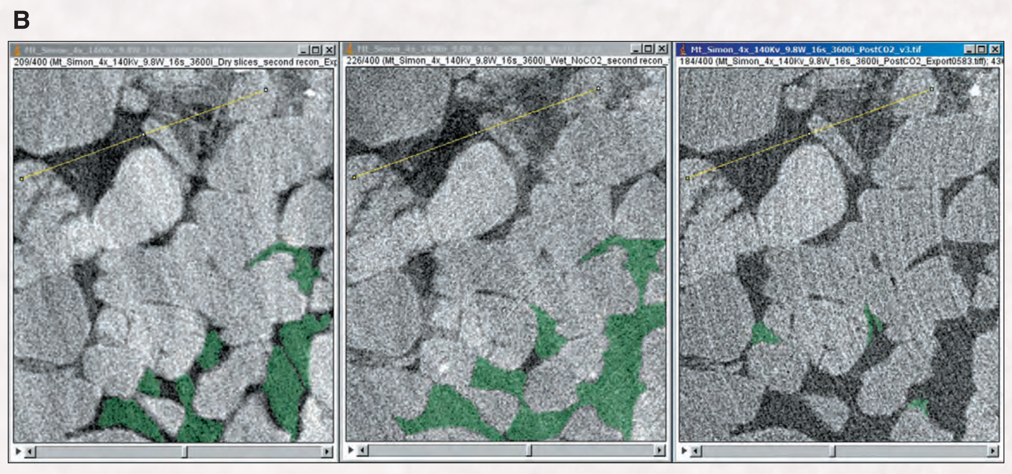

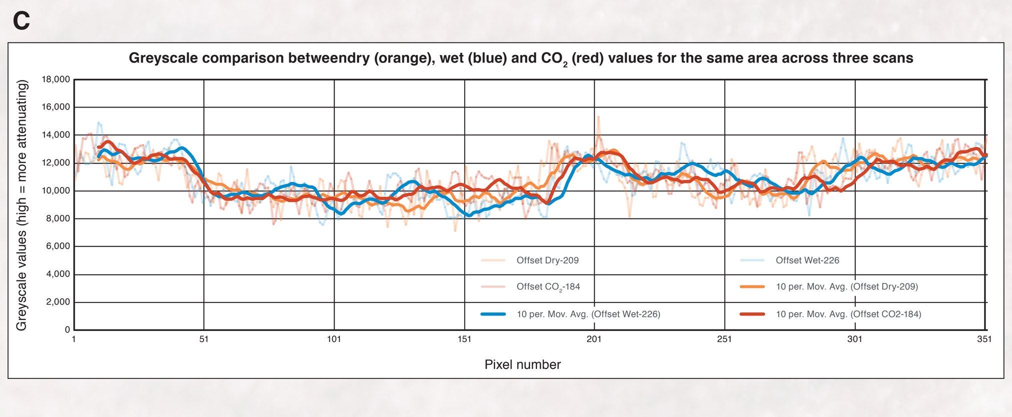

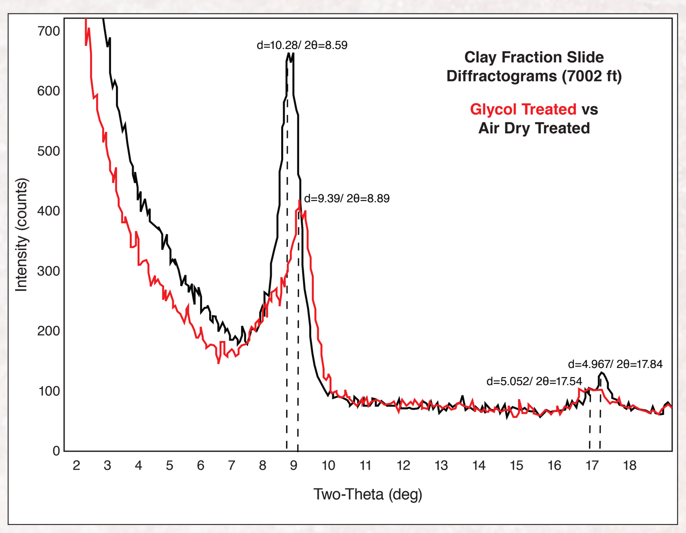

Figure 9. Diffractogram overlay of glycol treated (red) and air dried (black) clay fraction slides from 7,002 feet. There is no definitive low angle peak near 5°2θ, yet the ethylene glycol solvation has caused a change in the diffraction pattern indicating the presence of a smectite component. The small, broad reflection near 17.7°2θ (d=5.052 and d=4.967), coupled with the peak near 8.8°2θ (d=9.39 and d=10.28), indicates that the phase is illite/smectite (I/S). Using the position of the 17.7°2θ peak, it is estimated that the percent illite in the I/S is 90-95%. Note also the shift in the 8.8°2θ peak position between the air dried sample (d=10.28) and the glycol treated sample (d=9.39). The broad low angle shoulder, with a doublet peak on the 8.8°2θ also suggests long-range ordering (Moore & Reynolds 1997).

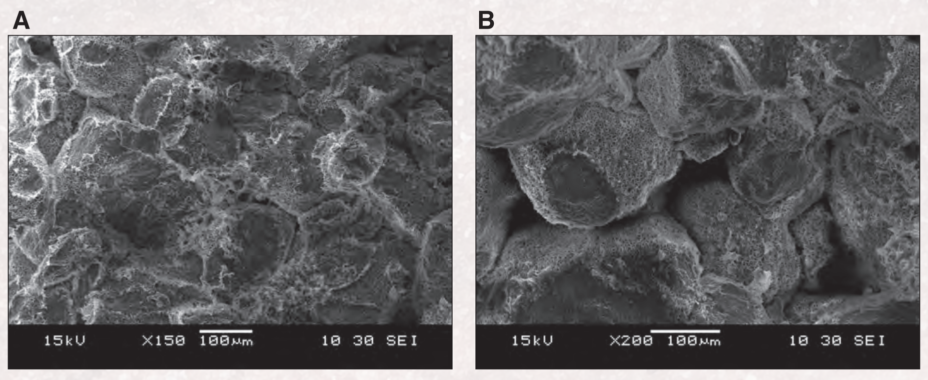

Figure 10. A: SEM photomicrograph of dry sample before CO_2-water flow through. Notice abundant clay filling pore space and coating grains. B: SEM photomicrograph after CO_2-water flow through. Notice thin clay coatings and relatively open pore space.

Experimental/Discussion

In an attempt to understand the impact of CO_2 on clay minerals and ultimately reservoir properties in the Mt. Simon, a CO_2-water flow through experiment was set up with in-situ micro-CT imaging of the sample. In order to speed up reaction of the 48-hour experiment at ambient temperature (Table 1) and 1,500 psi, DI water was used instead of brine. The sample was scanned three times: dry, saturated with DI water, and post CO_2-water flow through (Fig. 8). Comparison of the three scans suggest swelling of clay after water saturation and dissolution or flushing of clay post-CO_2-water flow through. Swelling may be explained by minor mixed layered illite-smectite (Fig. 9). Clay subtraction post-CO_2-water is confirmed by SEM imaging before and after the experiment (Fig. 10). Water chemistry before and after the experiment is in progress. With suggested dissolution of clay minerals during CO_2-water reaction, porosity and permeability of the Mt. Simon should increase (Fig. 11). Further characterization and experimentation is needed to understand CO_2-brine-rock interaction and long-term alteration of the rock as a result of CO_2 storage.

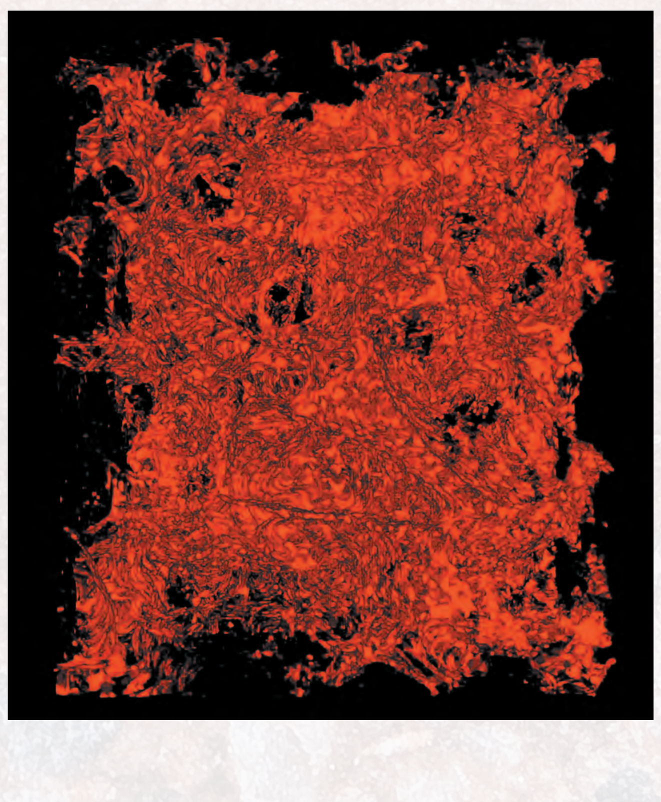

Figure 11. Micro-CT 3D reconstruction of pore space post-CO_2-water flow through. Unfortunately, the dry and saturated 3D reconstructions did not match, likely a result of detrital grain movement during clay subtraction. Thus, quantifying clay subtraction using CO_2 was not possible on this preliminary experiment.

References:

Bethke, C.M (1996) *Geochemical Reaction Modeling*. New York: Oxford University Press

Lasaga A. C. (1995) Fundamental approaches to describing mineral dissolution and precipitation rates. In *Reviews in Mineralogy Volume 31: Chemical Weathering Rates of Silicate 55 Minerals* (eds. A. F. White and S. L. Brantley). Mineralogical Society of America, Washington, D.C. pp. 23-86.

Moore, D. M. and R. C. Reynolds, Jr. (1997) X-ray Diffraction and the Identification and Analysis of Clay Minerals. 2nd Edition. Oxford University Press, Oxford

Storn R and K. Price (1997) Differential evolution A simple and efficient heuristic for global optimization over continuous spaces. *J Global Optim*; 11: 341-59

Yoksoulian, L. E., Freiburg, J.T., Butler, S.K., Berger, P.M., and Roy, W.R. (2013). Mineralogical Alterations during Laboratory-scale Carbon Sequestration Experiments for the Illinois Basin. Energy Procedia 37(0): 5601-5611.

Some of this work was supported as part of the Center of Geological Storage of CO_2, an Energy Frontier Research Center funded by the U.S. Department of Energy, Office of Sciences.